Records of Natural Products

Open Access
This article is licensed under CC-BY-NC-ND 4.0

www.acgpubs.org

SHORT REPORT

Rotatiridoid, a rare iridoid from *Phlomoides rotata* (Benth. ex Hook.f.) Mathiesen and its anti-inflammatory activity

Ling-Ping Zhu[1,3#], Da-Le Guo[2#], Yan-Fang Ran[2], Li Huang[2], Jie Li[2] and Jing Yang[1,2,3*]

[1]Institute of Herbgenomics, Chengdu University of Traditional Chinese Medicine, Chengdu 611137, China
[2]School of Pharmacy, Chengdu University of Traditional Chinese Medicine, Chengdu 611137, China
[3]School of Modern Chinese Medicine Industry, Chengdu University of Traditional Chinese Medicine, Chengdu 611137, China

Cite This: *Rec. Nat. Prod.* 2027, 21(2), e26094028

Read Online

Abstract: A rare iridoid featuring an unusual 3-*O*-8 bridged ether bond, named rotatiridoid (**1**), was obtained from *Phlomoides rotata* (Benth. ex Hook.f.) Mathiesen, along with five known analogues. Its structure was established by means of HRESIMS, 1D and 2D NMR experiments, and ECD calculations. When evaluated in LPS-stimulated RAW 264.7 macrophages, compound **1** displayed anti-inflammatory activity, suppressing the production of pro-inflammatory mediators such as NO and ROS at 7.5 μM.

Keywords: *Phlomoides rotata*, iridoid, anti-inflammatory, rotatiridoid

1 Plant Source

The aerial part of *Phlomoides rotata* (Benth. ex Hook.f.) Mathiesen was acquired from Sichuan Neautus Traditional Chinese Medicine Co., Ltd. Authentication was performed by Professor Guang-Zhi Wang of the School of Pharmacy, Chengdu University of Traditional Chinese Medicine. A voucher specimen (No. 202509012) has been deposited in the Laboratory of Traditional Chinese Medicine Chemistry at the School of Pharmacy, Chengdu University of Traditional Chinese Medicine.

2 Previous Studies

The aerial parts of *P. rotata* are primarily recognized for their capacity to promote blood circulation, stop bleeding, dissolve blood stasis, and alleviate pain (Cui et al., 2020). Traditionally, this plant has been employed in herbal medicine to address various conditions, including swelling and pain resulting from injuries such as falls and fractures, postoperative bleeding, rheumatism, joint pain, and gynecological bleeding (Li et al., 2010; Zhao et al., 2021). Phytochemical investigations of *P. rotata* have identified a diverse array of natural products characterized by distinct structural patterns, including iridoid glycosides, phenylethanoid glycosides, and flavonoids (Li et al., 2021; Ran et al., 2026; Zhu et al., 2027).

3 Present Study

The powdered aerial parts of *P. rotata* (30 kg) were extracted using 95% methanol. The extract was concentrated under reduced pressure, suspended in water, and subjected to column chromatography on D101 macroporous resin, which was eluted with a water–methanol gradient (0% to 100% methanol). The 30% methanol eluate, which was enriched in iridoids, was further separated on silica gel (200–300 mesh) using a methanol–water gradient (25:1 to 1:1, v/v), resulting in nine fractions (Fr.1–Fr.9).

Fraction 2 (Fr.2) was separated using a Sephadex LH-20 column with a solvent mixture of dichloromethane (DCM) and methanol (MeOH) in a 1:1 ratio, yielding subfractions Fr.2.1 to Fr.2.6. Subfraction Fr.2.4 underwent flash silica gel chromatography with a gradient of DCM to MeOH (100:0 to 0:100), resulting in subfractions Fr.2.4.1 to Fr.2.4.13. Subfraction Fr.2.4.6 was further purified using semi-preparative reverse-phase C_{18} high-performance liquid chromatography (RP-C_{18} HPLC) with a solvent composition of MeOH and H_2O (45:55, 10 mL/min), yielding subfractions Fr.2.4.6.1 to Fr.2.4.6.8. Additionally, subfraction Fr.2.4.6.4 was purified by semi-preparative RP-C_{18} HPLC with a different solvent ratio of MeOH to H_2O (40:60, 3 mL/min), leading to subfractions Fr.2.4.6.4.1 to Fr.2.4.6.4.5.

*Corresponding Author: Jing Yang.
Email: yangjingc@cdutcm.edu.cn
#These authors contributed equally to this work

Received: September 23, 2026
Revised: October 15, 2026
Accepted: October 16, 2026
Published: November 02, 2026

Copyright © 2026. Published by ACG Publications.

Table 1. The NMR data of **1**[a]

Position	δ_H (*J*, Hz)	δ_C, type
1	–	171.7, C
2	–	–
3	7.37, s	156.0, CH
4	–	108.2, C
5	3.25, d (4.0)	43.3, CH
6	4.05, d (6.0)	76.8, CH
7	3.81, d (6.0)	81.2, CH
8	–	88.3, C
9	3.11, d (4.0)	44.7, CH
10	1.55, s	18.4, CH_3
11	–	168.4, C
12	3.65, s	52.1, CH_3
13	3.71, s	51.8, CH_3

Note: a: measured in CD_3OD using a 600 MHz instrument.

Subsequently, subfraction Fr.2.4.6.4.3 underwent further purification via semi-preparative reverse-phase quaternary ammonium C18 high-performance liquid chromatography (RP-QA C18 HPLC) with a solvent mixture of MeOH and H_2O (26:74, 3 mL/min), resulting in three subfractions, from which **1** (Fr.2.4.6.4.3.1, 4.0 mg, t_R = 33.6 min) was isolated (Figure 1).

Fraction 3 (Fr. 3) was fractionated using C_{18} column chromatography, resulting in the isolation of fractions Fr.3.1 to Fr.3.8. Subsequently, Fr.3.5 was separated using a Sephadex LH-20 column with a DCM–MeOH solvent system (1:1), yielding fractions Fr.3.5.1 to Fr.3.5.4. From Fr.3.5.3, which underwent flash chromatography (DCM–MeOH, 100:0 to 0:100), fraction Fr.3.5.3.4 was further purified by semi-preparative RP-C_{18} HPLC, resulting in fractions Fr.3.5.3.4.1 to Fr.3.5.3.4.9. Fraction Fr.3.5.3.4.4, subjected to silica gel chromatography (DCM–MeOH, 8:1), produced fractions Fr.3.5.3.4.4.1 to Fr.3.5.3.4.4.4. Fraction Fr.3.5.3.4.4.2 was purified by RP-C_{18} HPLC, using a MeOH–H_2O solvent system (46:54), yielding fractions Fr.3.5.3.4.4.2.1 to Fr.3.5.3.4.4.2.3, while Fr.3.5.3.4.4.2.2 underwent further purification (ACN–H_2O, 25:75), resulting in **2** (15.1 mg, t_R = 23.4 min). Fraction Fr.3.5.3.4.3, processed through silica gel (DCM–MeOH, 8:1), yielded fractions Fr.3.5.3.4.3.1 to Fr.3.5.3.4.3.3. Fraction Fr.3.5.3.4.3.2 was purified by RP-C_{18} HPLC (MeOH–H_2O, 37:63), yielding **3** (10.7 mg, t_R = 28.6 min), while fraction Fr.3.5.3.4.3.2.2 underwent further purification (MeOH–H_2O, 39:61) to yield **5** (5.2 mg, t_R = 24.8 min). From Fr.3.5.4, which underwent flash chromatography (DCM–MeOH, 100:0 to 0:100), fraction Fr.3.5.4.3 was subjected to silica gel chromatography (DCM–MeOH, 40:1 to 0:100), producing fractions Fr.3.5.4.3.1 to Fr.3.5.4.3.4. Fraction Fr.3.5.4.3.2 was purified by RP-C_{18} HPLC (MeOH–H_2O, 55:45), yielding fractions Fr.3.5.4.3.2.1 to Fr.3.5.4.3.2.6, from which **4** (7.3 mg, t_R = 35.6 min), and **6** (12.2 mg, t_R = 24.2 min) were isolated through further RP-C_{18} HPLC purification.

Compound **1**: yellow gum; $[\alpha]_D^{25}$ = −90.0 (c = 0.03, MeOH); IR (KBr): 3311, 1636, 1443, 1217, 1100, 1017 cm^{-1}; UV(MeOH) λ_{max} 245 (2.34) nM; ECD (c 0.73 mM, MeOH) λ_{max} (Δε) 244 (−0.23) nm; HRESIMS *m/z* 295.0784 $[M + Na]^+$ (calcd. 295.0794). For details on the ^1H and ^{13}C NMR data, see Table 1.

Rotatiridoid (**1**) was isolated as a yellow gum. The HRESIMS ion peak at *m/z* 295.0784 $[M + Na]^+$ indicates the molecular formula of **1** should be $C_{12}H_{16}O_7$. The absorption in IR spectrum indicated the existence of hydroxyl (3311 cm^{-1}), and ester group (1636 cm^{-1}). The ^1H-NMR spectrum of **1** indicated the presence of an olefinic proton, two oxy-methines, two methoxy groups, two methines and a methyl. The ^{13}C NMR and HSQC spectra of **1** display 12 carbon resonances which classified two ester carbonyls (C-1 and C-11), a pair of olefinic carbons (C-3 and C-4), two oxy-methines (C-6, C-7), two methines (C-5, C-9), a sp^3 quaternary carbon (C-8), two methoxy signals (C-12 and C-13)

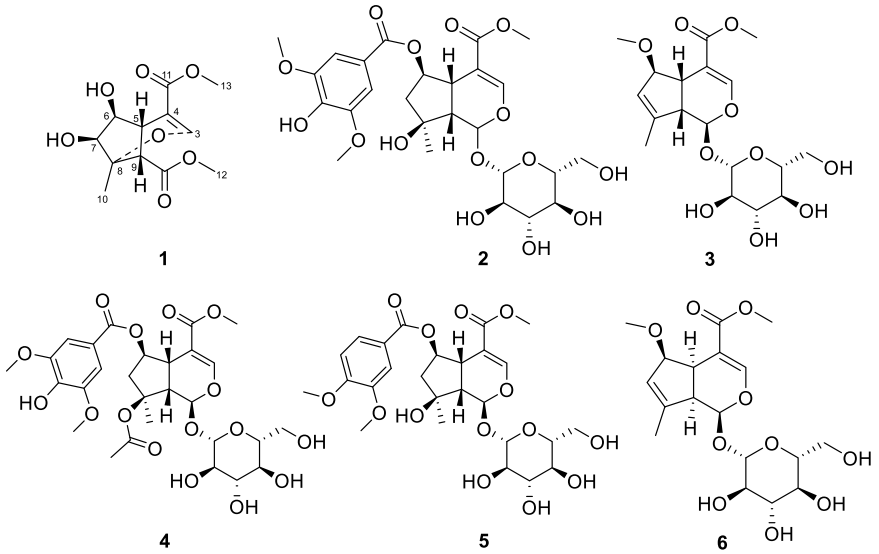


Figure 1. The structures of **1**–**6**

https://doi.org/10.25135/rnp.2609.4028
Rec. Nat. Prod. 2027, 21(2):e26094028

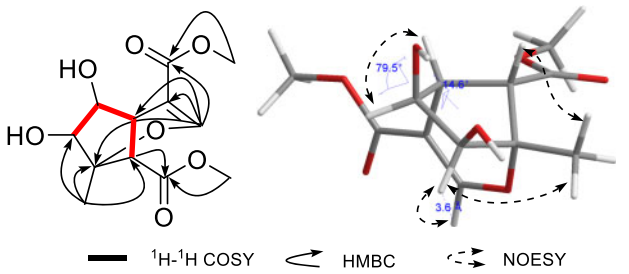


Figure 2. The key ^{1}H-^{1}H COSY, HMBC and NOESY correlations of **1**

and a methyl (C-10). The ^{1}H-^{1}H COSY correlations of H-9/H-5/H-6/H-7 along with HMBC correlations of H-3/C-4, 5, 8, 11; H-9/C-1; H-10/C-7, 8, 9; H-12/C-1 and H-13/C-11 generated the planar structure of **1** (Figure 2).

The relative configuration of **1** was deduced from the NOESY correlations observed between H-5/H-6, H-6/H-7, H-7/H-10, and H-9/H-10, as illustrated in Figure 2. This configuration results in a nearly 80-degree dihedral angle among H-5, C-5, C-6, and H-6 explaining the nearly zero coupling constant observed between these two protons (Figure 2). The relative configuration of the diol moiety is indicated to be *erythro*, as confirmed by the NOESY correlations of H-3/H-7 (Figure 2). The absolute configuration of the diol moiety was established by Snatzke's method (Zhang et al., 2026a). The positive Cotton effects observed at 300 nm (IV band) and 382 nm (II band) in the ICD spectrum of **1** indicate the positive torque angle between the complexation of **1** with $Mo_2(OAc)_4$ (Figure 3A) (Liu et al., 2026). Hence, the absolute configuration was established to be 5*S*, 6*S*, 7*S*, 8*S*, 9*S* which further confirmed through ECD comparisons (Figure 3B) (Han et al., 2026).

According to the SciFinder database, **1** was isolated as a new natural product. This compound is relatively novel, and we have not identified any structurally similar congeners. Among the currently reported compounds, the one with the closest structural resemblance is jatamanin L (Lin et al., 2010). The primary differences between jatamanin L and **1** include the oxidation and addition at carbon 3, which form a methyl ester moiety, as well as the formation of a double bond between carbons 4 and 11 in jatamanin L. In contrast, the newly reported compound (**1**) retains the characteristic double bond between carbons 3 and 4, typical of iridoids, and features an oxygen bridge connecting carbons 3 and 8. Notably, the two compounds exhibit significant differences in their NMR spectra; further details are provided in Table S1. In addition, **2**–**6** were identified as 6-*O*-syringyl-8-*O*-acetyl-shanzhiside methyl ester (**2**) (Tanaka et al., 1985), 6-methoxy-7,8-dehydropenstemonoside (**3**) (Li et al., 2017), 6-*O*-syringyl-8-hydroxy-shanzhiside methyl ester (**4**) (Tanaka et al., 1985), 6-*O*-veratroyl-shanzhiside methyl ester (**5**) (Kato et al., 2012), 5.9-epi-6-methoxy-7,8-dehydropenstemonoside (**6**) (Li et al., 2017).

To evaluate the anti-inflammatory activity of **1**, its cytotoxicity was initially assessed in macrophages (Xiao et al., 2026). As **1** did not exhibit significant cytotoxicity at concentrations ranging from 3.75 to 60 μM (Figure 4A), concentrations of 7.5, 15, and 30 μM were selected for subsequent anti-inflammatory experiments. NO and ROS are critical inflammatory molecules involved in LPS-induced macrophage activation (Liu et al., 2026; Nguyen et al., 2026). As illustrated in Figures 4B–4D, LPS stimulation markedly increased NO production and intracellular ROS accumulation, as well as upregulated the protein expression of iNOS and COX-2. Compared to dexamethasone (DXM) at a concentration of 30 μM, which served as a positive control (Zhang et al., 2026b), **1** significantly attenuated these LPS-induced inflammatory responses in a concentration-dependent manner. Collectively, these findings suggest that **1** exhibits *in vitro* anti-inflammatory activity and antioxidant capacity, potentially by suppressing the expression of inflammatory enzymes and reducing excessive NO and ROS production.

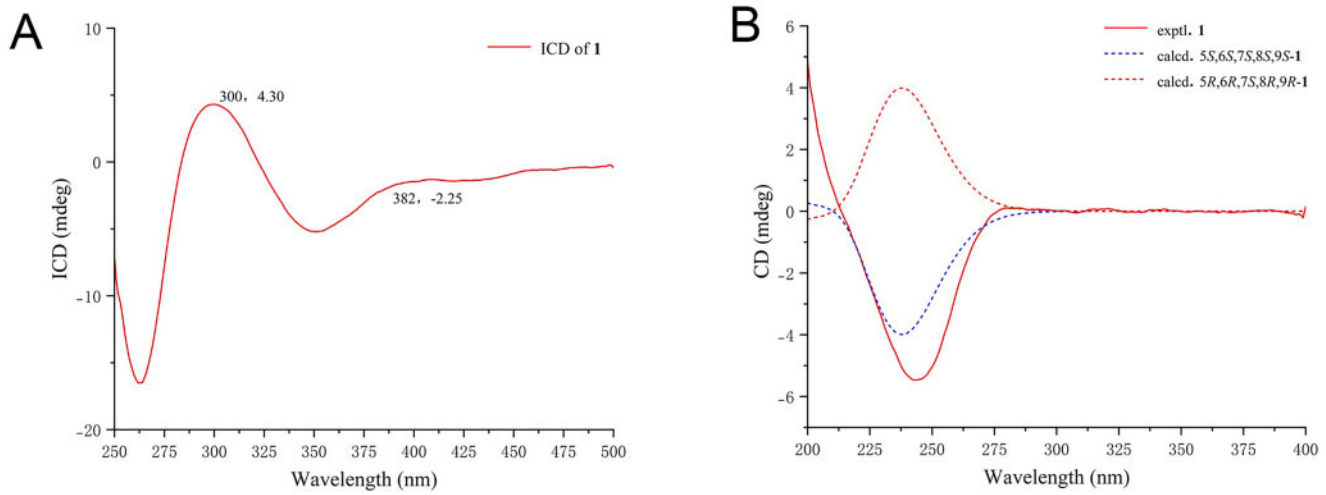


Figure 3. A. ICD spectrum of **1**; B. The calculated ECD curves and experimental ECD spectrum of **1**

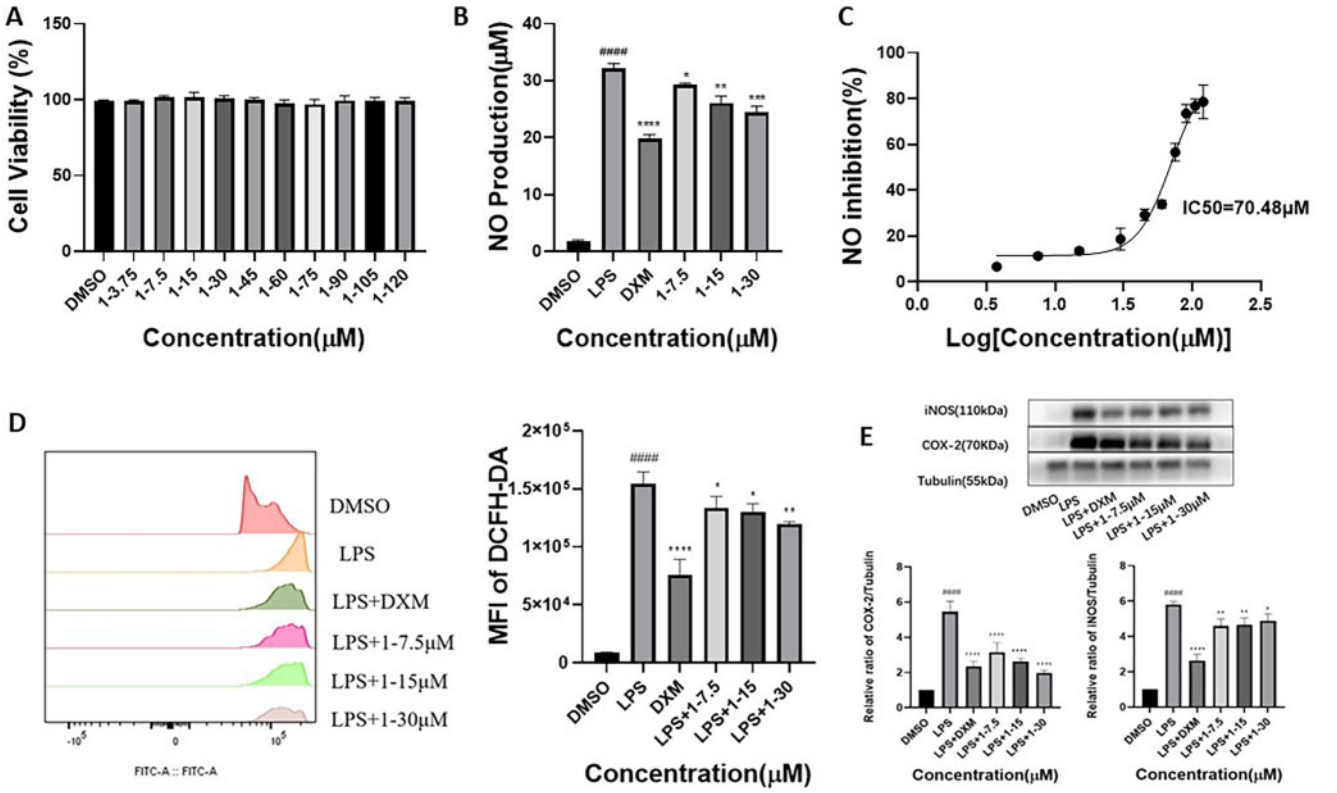


Figure 4. Anti-inflammatory activity of **1** on LPS-stimulated RAW264.7 macrophages. A: Viability of RAW264.7 cells following treatment with **1** at indicated concentrations. B: Suppressive effects of **1** on NO production in LPS-stimulated RAW264.7 cells; dexamethasone (DXM, 30 μM) served as a positive control. **C:** IC_{50} value for NO inhibition by **1**. **D**: Intracellular ROS levels detected by DCFH-DA staining and flow cytometry, with mean fluorescence intensity (MFI) quantified. **E**: Expression of iNOS and COX-2 detected by Western blot, with relative band intensities quantified against Tubulin as an internal control. All values are expressed as mean ± SD. $^{\#\#\#\#}p < 0.0001$ vs. DMSO group; $^{\#\#\#}p < 0.001$ vs. DMSO group; $^{****}p < 0.0001$, $^{***}p < 0.001$, $^{**}p < 0.01$, $^{*}p < 0.05$ vs. LPS group; ns, no significance.

Acknowledgement

Innovative Institute of Chinese Medicine and Pharmacy, Chengdu University of TCM is greatly appreciated for the CD and NMR measurements.

Funding Statement

This work was financially supported by the National Natural Science Foundation of China (grant number: 32271523), the Sichuan Provincial Administration of Traditional Chinese Medicine (grant number: 26MSZX560) and the Tianfu E'mei Talent Foundation for Young Scientists of Sichuan Province, China (grant number: No. 2969).

Author Contributions

Ling-Ping Zhu: Writing—original draft, Investigation, Data curation, Funding acquisition. Da-Le Guo: Data curation, Validation, Funding acquisition. Yan-Fang Ran: Investigation, Data curation. Li Huang: Data curation. Jie Li: Data curation. Jing Yang: Supervision, Validation, Writing—review & editing, Funding acquisition.

Availability of Data and Materials

The authors declare that the data supporting the findings of this study are available within the paper and its Supplementary Information files. Should any raw data files be needed in another format they are available from the corresponding author upon reasonable request. Source data are provided with this paper.

Artificial Intelligence (AI) Statement

The authors affirm that no Artificial Intelligence (AI) tools were employed in the preparation of this manuscript, which includes language editing, graphical abstract preparation, figure generation, or image editing.

Conflicts of Interest

The authors declare that they do not have any conflict of interest.

Supporting Information

Supporting information accompanies this paper on http://www.acgpubs.org/journals/records-of-natural-products.

https://doi.org/10.25135/rnp.2609.4028
Rec. Nat. Prod. 2027, 21(2):e26094028

ORCID

Ling-Ping Zhu: 0000-0001-6959-7755
Da-Le Guo: 0000-0003-3219-7066
Yan-Fang Ran: 0009-0005-6970-5441
Li Huang: 0000-0003-4193-6924
Jie Li: 0009-0009-8938-6301
Jing Yang: 0000-0002-6680-7486

References

Cui, Z. H., Qin, S. S., Zang, E. H., Li, C., Gao, L., Li, Q. C., Wang, Y. L., Huang, X. Z., Zhang, Z. Y. & Li, M. H. (2020). Traditional uses, phytochemistry, pharmacology and toxicology of *Lamiophlomis rotata* (Benth.) Kudo: A review. *RSC Advances*, *10*, 11463. DOI: 10.1039/d0ra01050b.

Han, M. Q., Zhang, J. C., Zhao, Y. J., Liu, Y. F., Zhu, H. J., Pittman, C. U. & Cao, F. (2026). A marine-derived meroterpenoid inhibits colorectal cancer via PI3K pathway modulation in mice. *Marine Life Science & Technology*, *8*(3), 767–782. DOI: 10.1007/s42995-026-00356-7.

Kato, L., de Oliveira, C. M. A., Melo, M. P., Freitas, C. S., Schuquel, I. T. A. & Delprete, P. G. (2012). Glucosidic iridoids from *Molopanthera paniculata* Turcz. (Rubiaceae, Posoquerieae). *Phytochemistry Letters*, *5*, 155–157. DOI: 10.1016/j.phytol.2011.11.013.

Li, Y., Li, F., Zheng, T. T., Shi, L., Zhang, Z. G., Niu, T. M., Wang, Q. Y., Zhao, D. S., Li, W. & Zhao, P. (2021). Lamiophlomis herba: A comprehensive overview of its chemical constituents, pharmacology, clinical applications, and quality control. *Biomedicine & Pharmacotherapy*, *144*, 112299. DOI: 10.1016/j.biopha.2021.112299.

Li, X. H., Lu, L. H., Li, X. H., Li, Y. B., Zha, Y. F., Fu, D. H., Mei, S. X., Cui, T., Wang, J. K. & Zhu, Z. Y. (2017). Iridoid glycosides from *Phlomis likigangensis* with free-radical scavenging activity. *Tetrahedron Letters*, *58*(46), 4395–4399. DOI: 10.1016/j.tetlet.2017.10.020.

Li, M. X., Shang, X. F., Zhang, R. X., Jia, Z. P., Fan, P. C., Ying, Q. & Wei, L. L. (2010). Antinociceptive and anti-inflammatory activities of iridoid glycosides extract of *Lamiophlomis rotata* (Benth.) Kudo. *Fitoterapia*, *81*(3), 167–172. DOI: 10.1016/j.fitote.2009.08.018.

Lin, S., Chen, T., Liu, X.-H., Shen, Y.-H., Li, H.-L., Shan, L., Liu, R.-H., Xu, X.-K., Zhang, W.-D. & Wang, H. (2010). Iridoids and lignans from *Valeriana jatamansi*. *Journal of Natural Products*, *73*(4), 632–638. DOI: 10.1021/np900795c.

Liu, M.-D., Huang, L. J., Lei, H.-R., Wang, Y.-J., Hu, Y.-J., Huo, X.-Y., Li, C.-C., Huang, L., Zhao, L.-L., Zhang, M.-Z., Gu, Y.-C., Shyy, M., Sihota, A., Wang, D., Guo, D.-L. & Deng, Y. (2026). Discovery of notoprenylate F from *Notopterygium incisum* (Qianghuo) as a PPARγ agonist with potent anti-inflammatory activity through HTS^2. *Marine Life Science & Technology*, *8*(3), 828–840. DOI: 10.1007/s42995-026-00358-5.

Nguyen, H. T., To, P. M., Pham, T. N., Nguyen, D. M. T., Nguyen, L., Duong, T. H., Nguyen, T. H. T., Nguyen, N. H., Sichaem, J. & Funnimid, N. (2026). Nitric oxide inhibitory compounds from Thai medicinal plants *Averrhoa bilimbi* and *Schinus terebinthifolia*. *Records of Natural Products*, *20*(1), e25073593. DOI: 10.25135/rnp.2507.3593.

Ran, Y. F., Huang, L., Li, J., Zhao, L. L. & Guo, D. (2026). Three undescribed iridoid glycosides from *Lamiophlomis rotata* and their anti-inflammatory activity. *Chinese Journal of Organic Chemistry*. DOI: 10.6023/cjoc202605008.

Tanaka, T., Tanaka, O., Lin, Z. W. & Zhou, J. (1985). Sweet and bitter principles of the Chinese plant drug, Bai-Yun-Shen: Revision of the assignment of the source plant and isolation of two new diterpene glycosides. *Chemical and Pharmaceutical Bulletin*, *33*(10), 4275–4280. DOI: 10.1248/cpb.33.4275.

Xiao, J., Zou, D.-Z., Zeng, H.-L., Hu, Y.-B., Zhang, S.-H. & Cheng, F. (2026). A new isoflavone from the ethyl acetate extracts of *Apios fortunei* Maxim and anti-inflammatory activity. *Records of Natural Products*, *20*(1), e25063553. DOI: 10.25135/rnp.2506.3553.

Zhang, B.-D., Liu, L.-H., Wang, S., Sun, X.-Q., Zi, G.-R., Hong, K., Sun, L.-Y. & Liu, L. (2026a). Discovery of antimicrobial citrinin dimers from the mangrove-derived fungus *Penicillium citrinum*. *Phytochemistry*, *243*, 114739. DOI: 10.1016/j.phytochem.2025.114739.

Zhang, C.-Y., Yang, L.-J., Jiang, L.-S., Mu, Y.-T., Mao, X.-L., Liu, Q., Deng, F. & Guo, D.-L. (2026b). HR-LC/MS guided separation and identification of acyl-migrated sucrose esters from Physalis Calyx seu Fructus. *Phytochemical Analysis*, *37*, 85–99. DOI: 10.1002/pca.70028.

Zhao, X. H., Jiang, S. R., Dong, Q., Dong, J., Liu, Z. G., Han, H. P., Tao, Y. D. & Yue, H. L. (2021). Anti-rheumatoid arthritis effects of iridoid glucosides from *Lamiophlomis rotata* (Benth.) kudo on adjuvant-induced arthritis in rats by OPG/RANKL/NK-κB signaling pathways. *Journal of Ethnopharmacology*, *266*, 113402. DOI: 10.1016/j.jep.2020.113402.

Zhu, L. P., Guo, D. L., Ran, Y. F., Huang, L., Li, J. & Yang, J. (2027). A new iridoid glycoside with anti-inflammatory activity from *Lamiophlomis rotata*. *Records of Natural Products*, *21*(1), e26073980. DOI: 10.25135/rnp.2607.3980.